
Advanced Structural and Functional Materials Design

Edited by

**Yukichi Umakoshi
Shinji Fujimoto**

ttp TRANS TECH PUBLICATIONS

Advanced Structural and Functional Materials Design

Edited by
Yukichi Umakoshi
Shinji Fujimoto

Advanced Structural and Functional Materials Design

Proceedings of the International Symposium on
Advanced Structural and Functional Materials Design,
Osaka, Japan, November 10-12, 2004

Edited by

Yukichi Umakoshi and Shinji Fujimoto

 *Scientific.Net*

Copyright © 2005 Trans Tech Publications Ltd, Switzerland

All rights reserved. No part of the contents of this publication may be reproduced or transmitted in any form or by any means without the written permission of the publisher.

Trans Tech Publications Ltd
Kapellweg 8
CH-8806 Baech
Switzerland
<https://www.scientific.net>

Volume 512 of
Materials Science Forum
ISSN print 0255-5476
ISSN web 1662-9752

Full text available online at <http://www.scientific.net>

Distributed worldwide by

Trans Tech Publications Ltd
Kapellweg 8
CH-8806 Baech
Switzerland
Phone: +41 (44) 922 10 22
Fax: +41 (44) 922 10 33
e-mail: sales@scientific.net

Table of Contents

Thoughts on the Occasion of the Second Transformation in Materials Science M. Meshii	1
Interfaces and Properties of Advanced Materials V. Paidar	5
Observation of Lattice Defects and Nondestructive Evaluation of Fatigue Life in FeAl and Ni₃Al Based Alloy by Means of Magnetic Measurement Y. Umakoshi and H.Y. Yasuda	13
Metallurgical and Mechanical Heterogeneity in Weld Materials Considering Multiple Heat Cycles and Phase Transformation M. Toyoda, M. Mochizuki and Y. Mikami	19
Pseudoelasticity in Fe₃Al Single Crystals under Cyclic Loading H.Y. Yasuda, K. Yamaoka and Y. Umakoshi	25
Damage Mechanism for Controlling Ductile Cracking of Structural Steel with Heterogeneous Microstructure M. Ohata and M. Toyoda	31
Superplastic Deformation and Thermal Crystallization Behavior of Supercooled Liquid in Zr-Ni Based Metallic Glass T. Nagase, M. Nakamura and Y. Umakoshi	37
Effect of Cooling Rate on As-Cast Texture of Low-Carbon Steel Strips During Rapid Solidification P.G. Xu, F.X. Yin and K. Nagai	41
Microstructural Evolution during Simple Heavy Warm Deformation of a Low-Carbon Steel S.V.S. Narayana Murty, S. Torizuka and K. Nagai	49
Effect of Hydrogen on the Fracture Behavior of High-Strength Cr-Mo Steel M.Q. Wang, E. Akiyama and K. Tsuzaki	55
Evaluation Method for Fracture Mechanics-Based Material Toughness from Charpy Impact Test Y. Takashima, M. Ohata and F. Minami	61
Temperature and Orientation Dependence of Fracture Behavior of Directionally Solidified Duplex-Phase Crystals Composed of Ni₃X-Type Intermetallic Compounds K. Hagihara, N. Yokotani and Y. Umakoshi	67
Microstructural Evolution in 36%Ni Austenitic Steel during the ARB Process B.L. Li, N. Tsuji and Y. Minamino	73
Fine-Grained Structure Formation in 7475 Al Alloy during Hot Multidirectional Forging A. Goloborodko, O. Sitdikov, H. Miura and T. Sakai	79
Tensile Deformation Behaviors of Ultrafine Grained Al-Fe-Si Alloy Sheets H.W. Kim, S.B. Kang, N. Tsuji and Y. Minamino	85
EBSD and TEM Characterization of Ultrafine Grained High Purity Aluminum Produced by Accumulative Roll-Bonding N. Kamikawa, X. Huang, N. Tsuji, N. Hansen and Y. Minamino	91
Acetate and Chloride Effects on Hydrogen Production across Crevices T. Sundararajan, E. Akiyama and K. Tsuzaki	97
Process of the One-Dimensional Motion of Small Interstitial-Type Dislocation Loops in Iron K. Arakawa and H. Mori	103
Effect of Electron Irradiation on Nanocrystallization of Fe-Nd-B Amorphous Alloys A. Nino, T. Nagase and Y. Umakoshi	107
Isothermal Oxidation Behavior of Ru Modified Aluminide Coating on a Fourth Generation Single Crystal Superalloy Y. Matsuoka, K. Chikugo, T. Suzuki, Y. Matsunaga and S. Taniguchi	111
Variant Selection of Plate Martensite in Fe-28.5at.%Ni Alloy H. Kitahara, M. Ueda, N. Tsuji and Y. Minamino	117
Internal Stress Field in Ultrafine Grained Aluminium Fabricated by Accumulative Roll-Bonding R. Ueji, J. Taniguchi, N. Sumida, K. Tanaka and N. Tsuji	123

Tailored Electrochemical Surface Modification of Semiconductors P. Schmuki	129
Application of Large Magnetocaloric Effects in Itinerant-Electron Metamagnets to Cooling Systems K. Fukamichi, A. Fujita and S. Fujieda	137
Ferromagnetic Shape-Memory Alloys A. Planes and L. Mañosa	145
Development of Photonic Fractals as New Functionally Structured Materials for Electromagnetic Wave Control Y. Miyamoto, S. Kirihara, M.W. Takeda, K. Honda and K. Sakoda	153
Behaviors of Nonequilibrium Carriers in Er, O-Codoped GaAs for 1.5μm Light-Emitting Devices with Extremely Stable Wavelength Y. Fujiwara, A. Koizumi, K. Nakamura, M. Suzuki, Y. Takeda and M. Tonouchi	159
Magnetism of Ultrathin Fe Films in the Vicinity of Transition from Ferromagnetism to Superparamagnetism Y. Shiratsuchi, Y. Endo and M. Yamamoto	165
Magnetization Chirality of Ni-Fe and Ni-Fe/Mn-Ir Asymmetric Ring Dots for High-Density Memory Cells I. Sasaki, R. Nakatani, T. Yoshida, K. Otaki, Y. Endo, Y. Kawamura, M. Yamamoto, T. Takenaga, S. Aya, T. Kuroiwa, S. Beysen and H. Kobayashi	171
Change of Interlayer Exchange Coupling between the Adjacent Magnetic Transition Metal Layers across a Rare-Earth Metal Layer by Hydrogenation Y. Endo, T. Sato, T. Kaneko, Y. Kawamura and M. Yamamoto	177
Magnetic Phase Diagram in Layered Perovskite Manganite $\text{La}_{2-2x}\text{Sr}_{1+2x}\text{Mn}_2\text{O}_7$ ($0.313 \leq x \leq 0.350$) T. Murata, T. Terai, T. Fukuda and T. Kakeshita	183
Martensitic Transformation of Ni-Mn-Ga Alloys under Magnetic Field and Hydrostatic Pressure J.H. Kim, T. Fukuda and T. Kakeshita	189
Magnetocrystalline Anisotropy and Twinning Stress of 10M and 2M Martensites in Ni-Mn-Ga System N. Okamoto, T. Fukuda, T. Kakeshita and T. Takeuchi	195
Influence of Magnetic Field Direction and Temperature on Rearrangement of Martensite Variants in Fe-31.2at.%Pd T. Sakamoto, T. Fukuda and T. Kakeshita	201
Anodic Porous Zirconium Oxide Prepared in Sulfuric Acid Electrolytes H. Tsuchiya, J.M. Macak, I. Sieber and P. Schmuki	205
Surface Properties of Ag-Cu-Zr Liquid Alloys in Relation to the Wettability of Boride Ceramics R. Novakovic, M.L. Muolo, E. Ricci, E. Ferrera, D. Giuranno, F. Gnecco and A. Passerone	211
Low Temperature Synthesis of TiO_2 / SrTiO_3 Films on Ti Substrate M. Ueda, D. Ohzaike and S. Otsuka-Yao-Matsuo	217
Microstructures Formed by Charge Ordering Transition in $\text{Pr}_{0.55}\text{Ca}_{0.45}\text{MnO}_3$ and $\text{Nd}_{0.5}\text{Sr}_{0.5}\text{MnO}_3$ T. Terai, N. Tamai, T. Fukuda and T. Kakeshita	223
Strong Localization of Electromagnetic Wave in Ceramic/Epoxy Photonic Fractals with Menger-Sponge Structure S. Kirihara, M.W. Takeda, K. Sakoda, K. Honda and Y. Miyamoto	227
Stability of the B2-Type Structure of Ti-Ni-Fe and Ti-Ni-Co Shape Memory Alloys M.S. Choi, J. Ogawa, T. Fukuda and T. Kakeshita	233
Design of Automatic Matching System for Very High Frequency Plasma-Enhanced Processes Y. Yoshizako and D. Matsuno	239
Recent Development of New Alloys for Biomedical Use T. Hanawa	243
Electrochemical Characterization of Ti and Ti Base Alloys under Simulated Body Fluid Environment S. Fujimoto, H. Kusu, S. Katsuma, M. Sakamoto and Y.C. Tang	249

Crystallographic Approach to Regenerated and Pathological Hard Tissues T. Nakano, T. Ishimoto, J.W. Lee, Y. Umakoshi, M. Yamamoto, Y. Tabata, A. Kobayashi, H. Iwaki, K. Takaoka, M. Kawai and T. Yamamoto	255
Role of Stress Distribution on Healing Process of Preferential Alignment of Biological Apatite in Long Bones T. Ishimoto, T. Nakano, Y. Umakoshi, M. Yamamoto and Y. Tabata	261
Role of Osteoclast in Preferential Alignment of Biological Apatite (BAP) in Long Bones J.W. Lee, T. Nakano, S. Toyosawa, N. Ijuhin, Y. Tabata, M. Yamamoto and Y. Umakoshi	265
Crystal Orientation in High Magnetic Field C.Y. Wu, S.Q. Li, Y. Murakami, K. Sassa and S. Asai	269
Microstructural Tailoring of Open-Pore Microcellular Aluminium by Replication Processing J. Despois, A. Marmottant, Y. Conde, R. Goodall, L. Salvo, C. San Marchi and A. Mortensen	281
Fabrication of Porous Aluminium and Copper Media by Using Monotectic Solidification under a Magnetic Field H. Yasuda, I. Ohnaka, B.K. Dhindaw, S. Fujimoto, N. Takezawa, T. Tamayama, A. Tsuchiyama, T. Nakano and K. Uesugi	289
Fabrication and Properties of Porous Materials with Directional Elongated Pores H. Nakajima, S.K. Hyun, M. Tane and T. Nakahata	295
Convection in Weld Pool under Microgravity and Terrestrial Conditions H. Fujii, N. Sogabe and K. Nogi	301
Advanced Eco-Materials Processing from By-Products T. Tanaka, S. Maeda, N. Takahira, N. Hirai and J.H. Lee	305
Novel Method Determining Contact Angle of Liquid Au on Solid Al₂O₃ Single Crystal (0001) Surface at 1373K J.H. Lee, H. Ishimura and T. Tanaka	309
Study of Microstructure in Surface-Melted Region of Ni-Base Single Crystal Superalloy CMSX-4 Y. Fujita, K. Saida and K. Nishimoto	313
Design of Lubricants Using Waste Slag in Large Strain Addition Strip Processing for Ultrafine-Grained Steels M. Nakamoto, J.H. Lee and T. Tanaka	319
Measurement and Analysis of Vibration Damping Capacity of Lotus-Type Porous Magnesium Z.K. Xie, S.K. Hyun, Y. Okuda and H. Nakajima	325
Extended Effective-Mean-Field Analysis for Electrical Conductivity of Lotus-Type Porous Nickel M. Tane, S.K. Hyun and H. Nakajima	331
Fabrication and Tensile Properties of Lotus-Type Porous Iron and SUS304L Stainless Steel S.K. Hyun, T. Ikeda, M. Tane and H. Nakajima	337
Analysis of Second Harmonic Pulse Distortion Induced by Repetitive Irradiation K. Nomura, E. Ohmura and I. Miyamoto	343
Femtosecond Laser Synthesis of the High-Pressure Phase of Iron T. Sano, O. Sakata, E. Ohmura, I. Miyamoto, A. Hirose and K.F. Kobayashi	349
Interfacial Microstructure and Joint Strength of Sn-Ag and Sn-Ag-Cu Lead Free Solders Reflowed on Cu/Ni-P/Au Metallization A. Hirose, T. Hiramori, M. Ito, Y. Tanii and K.F. Kobayashi	355
Enhancement of Reaction of Zinc on Superficially Nanocrystallized IF Steel by Near Surface-Severe Plastic Deformation Y. Minamino, N. Tsuji, Y. Koizumi, Y. Nakamizo, M. Sato, T. Shibayanagi and M. Naka	361
Influence of Resin Viscosity and Filler Volume on Self-Organized Micro Interconnection K. Yasuda, K. Ohta and K. Fujimoto	367
Effective Heat Transfer Analysis by Mesh Superposition Method F. Kubo, M. Zako and T. Kurashiki	373
Application of Numerical Simulation Considering the Effect of Phase Transformation to the Estimation of Hardness Distribution in Welds Y. Mikami, M. Mochizuki, T. Nakamura, K. Hiraoka and M. Toyoda	379

Bonding of Various Metals Using Ag Metallo-Organic Nanoparticles-A Novel Bonding Process Using Ag Metallo-Organic Nanoparticles- E. Ide, S. Angata, A. Hirose and K.F. Kobayashi	383
Effect of Threads on Tool in Friction Stir Welding of Aluminum Alloys H. Fujii, L. Cui, M. Maeda, Y.S. Sato and K. Nogi	389
Fundamental Measurements of the Friction on an Atomically-Flat Terrace of Au(100) in Sulfuric Acid Solution under Potential Control Using Electrochemical Atomic Force Microscope N. Hirai, T. Tooyama and T. Tanaka	395
Microscopic Structure of Water Flow through Carbon Nanotubes I. Hanasaki and A. Nakatani	399

Thoughts on the Occasion of the Second Transformation in Materials Science

M. Meshii

Department of Materials Science and Engineering,
The McCormick School of Engineering and Applied Science, Northwestern University,
Evanston, IL 60208-3108 U.S.A.

Keywords: hard materials, soft materials, metallurgy, interdisciplinary

Abstract. The discipline of Materials Science is, we believe, in the midst of the second transformation. The research and education of most of the Materials Science and Engineering departments in the United States have traditionally emphasized hard materials. The recent surge in research of soft materials and our perceptions that the Materials Science Methodology (both experimental and numerical) holds the advantage in the research of the soft materials prompt us to expand the area of soft materials at the expense of hard materials. Clearly the struggle between the two types of materials will continue for some time to come. The current struggle in weighting will be described in an historical fashion comparing it to the struggle in the first transformation that took place in the 1950's and 1960's.

Introduction

Materials Science became an academic discipline mostly in engineering schools of universities and possesses unique characteristics. Depending on who describes it, adjectives such as "interdisciplinary", "dynamic" and "applied" are employed. As a part of an engineering school, its mission must include the rapid and effective response to the technical and societal needs and, at the same time, it must maintain a very high academic standard both in education and research. Because it is a relatively new discipline, and is interdisciplinary and dynamic, it is in striking contrast to more traditional disciplines such as biology, chemistry and physics. In this short manuscript, its emergence, i.e., the first transformation, development, and the second transformation are briefly reviewed to characterize Materials Science.

Emergence and Development of Materials Science

Many Materials Science (and Engineering) departments are transforms from Metallurgy and other related departments. The stimuli for the first transformation came from academic fields as well as technological needs. The academic stimulus was impressive advances in the area of solid state physics both in application of theories and experimental achievements, enabling metallurgists to quantify and predict their observations. The discoveries and theoretical developments in 1940's and 54's in the area of phase transformation, diffusion and lattice imperfections truly ignited the passion of young researchers in metallurgy to utilize the new approach to their subjects. World War II stimulated the needs of new materials and necessitated scientists and engineers from different disciplines to collaborate in urgent and important projects such as Manhattan Project [1]. The subsequent Cold War further promoted such interdisciplinary collaboration again with a sense of urgency this again with a sense of urgency. People, who had been involved in the collaboration also realized the advantage and started to utilize more and more in their field. The rapid technological developments in the post war period also demanded engineers and scientists with a broad knowledge of various classes of materials such as ceramics, semiconductors and polymers in additions to metals. The concepts of Materials Science took a shape in this background and the first department under the concept was established in 1955. This trend, although initially questioned, gradually gained strength in the 1960's. In the

following twenty years, the discipline of Materials Science and Engineering gained firm recognition and appeared to mature, but it was destined to be dynamic. This may contradict the belief of some practitioners who consider stability to its curriculum and static maturity of the subject as the condition of an established discipline [2]. The present author believes that the disciplines in engineering schools must be dynamic, responding as rapidly as possible to the need of society and industries. In this sense, Materials Science departments can spearhead the current effort of many engineering schools in their effort to innovate education and research. There is also a strong trend both in research and education of engineering that interdisciplinary activities are increasing.

Strength of Discipline of Materials Science

It has been repeatedly pointed out that Materials Science is a science to study structure and property of materials and to establish their relationship. Materials Science employs most effort in structure determination in molecular and atomic levels, utilizing best instruments available and developing sophisticated techniques. We train our students to be the best structure analysts. At the same time materials scientists are advanced in property measurements. Then, they are trained to correlate the structure observed to the property determined. In addition, with the recent advancement in numerical analysis with computers, specialists have been trained to predict how molecules and atoms are arranged in materials under various conditions numerically. The processing techniques are continuously developed to produce these structures. All of these specializations have been acquired within the initial framework of Materials Science, working on metals, ceramics, semiconductors and polymers. Furthermore, a typical Materials Science department is very interdisciplinary in the composition of faculty members and graduate students. They are trained to adjust with and take advantage of different scientific approach and different terminologies inherent with different disciplines. In other words, Materials Scientists are expert in interdisciplinary activities.

The strength mentioned above is fully demonstrated in investigation of materials, but nearly exclusively to hard materials until ten years ago except more traditional investigation of polymeric materials. The situation has started to change with increasing momentum.

Second Transformation

The revolutionary development in Molecular Biology and Biochemistry enabled to process and analyze molecular materials with precise molecular control. The methodology such as self assembly of nano fibers has been utilized to design materials with various properties that are suitable in biological and medical applications. The biological structure can be determined and can be mimicked to produce synthesized biological materials. It has been speculated and demonstrated in a preliminary fashion that parts of biological bodies can be repaired and /or replaced by the materials thus developed. Materials scientists, demonstrating possibilities of repairing spinal cords and bones, have reported preliminary studies.

The demand and funding from medical and pharmaceutical industries would certainly accelerate these types of investigations. Students are eager to get involved in research in these areas. The prize is huge. Substantial developments are eminent. Material Scientists are only one of many players competing for the prize. The competition is coming from many disciplines. The question is "do we have an edge" in this competition. The time will tell.

Closing Remarks

Materials Science with characteristics of "dynamic" and "interdisciplinary" will move into the field of soft material - biological materials and other molecular materials, utilizing its expertise in structure, property and processing. The competition with other discipline will be fierce and hard. The

outcome will not likely to be "winner takes all". Multiple disciplines will probably contribute to the research with their different strength. The interdisciplinary collaboration among them will be essential.

Another hurdle to encompass this new area is the inclusion of bio and soft materials in the core curriculum of materials Science. It is currently debated and will be published soon.

Reference

- [1] Morris E. Fine and Peter W. Voorhees: To be published in Daedalus.
- [2] Bernadette Bensande-Vincent and Arne Hessenbruch: Nature Materials 3, 345-347 (2004).

Interfaces and properties of advanced materials

V. Paidar

Institute of Physics ASCR, Na Slovance 2, 182 21 Praha 8, Czech Republic

paidar@fzu.cz

Keywords: Interfaces, magnetic properties, lattice misfit, grain boundary classification.

Abstract. Internal interfaces are decisive for many properties of materials. Both functional and structural properties of interfaces are briefly reviewed on selected examples. Approaches to the grain boundary classification are discussed in the context of the complex relationship between microstructure and material properties. Implications for grain boundary engineering are mentioned.

Introduction

The properties of materials are affected to a large extent by the internal interfaces. These planar defects of the ordered crystal structure are buried in the material interior, and are thus less accessible to various experimental techniques than the external surfaces. In general, the interfaces play a crucial role in diverse fields such as transportation, energetics, electronics, medicine etc. Hence the study of their properties is a cross-disciplinary task. Let us restrict our considerations here only to physical and chemical properties that are directly related to the interface atomic structure, and only to solid state, i.e., the interfaces between liquid and gas phases equally important will be excluded despite their technological significance.

Due to short-range stress field the influence of interfaces is primarily based on their atomic structure. Special character of grain boundary properties follows from the nature of atomic arrangements in the boundary cores, from the interfacial dislocation content and from the boundary mobility. All those aspects of boundary behaviour are strongly influenced by the boundary chemistry including various segregation phenomena.

The interfaces are both sources and sinks of point defects as vacancies or imperfections and affect thus the properties sensitive to such defect concentrations. Since the diffusion along the interfaces is faster than inside the perfect crystal, plastic deformation at elevated temperatures can occur under certain conditions by the interfacial diffusion. Segregation of impurities is decisive for the cohesive properties of interfaces and can be a principal cause of intergranular fracture. Moreover, the interfaces are preferential sites for precipitation and the interfacial structure can be favourable for initiation of new phase formation.

The interfaces can be strong obstacles for dislocation motion. Consequently, the plastic deformation is directly affected by the interfacial arrangement that can be substantially modified by thermo-mechanical material processing.

The most close-packed atomic planes can be taken as the starting building elements for the construction of the grain boundary classification. These planes represent the facets of small atomic clusters with the three atoms at the shortest distances defining the plane orientation. Such planes have the lowest density of irregularities.

The number of papers containing data on different grain boundaries is very limited. A large number of good quality bicrystals is needed for such measurements and their preparation is a requisite condition for systematic research. Let us mention one example here - structure, energy and fracture stress were studied on molybdenum bicrystals [1-4]. Two series of grain boundaries were investigated: symmetrical tilt boundaries with the [110] rotation axis and twist boundaries on the {110} plane. The specimens were tested by four-point bending at the temperature of 77 K much

lower than the ductile-brittle transition in molybdenum polycrystals. The fracture always initiated at grain boundaries.

This paper is organized in the following way. First the magnetic properties of homogeneous thin films will be discussed, then the dislocation structure of interfaces will be dealt with, in the next section a revised version of grain boundary classification will be described and finally, its consequences for the grain boundary engineering will be assessed.

Magnetism in Thin Films

To study magnetism is not exciting only because of its technologically important applications in magnetic recording but it is still attractive as physical phenomenon itself. As an example of the functional property affected by interfaces, let us discuss magnetic states in thin films.

The atomic magnetic moment is very sensitive to the atom surrounding, it is the highest for the isolated atom, decreases for one-dimensional atomic chain, further goes down for atomic mono-layer and the atoms on the free surface, and finally, it reaches a bulk value for the ordered crystal. The calculated values for iron [5] and critically assessed values for cobalt [6] are summarized in Table 1. The atomic moment of two-dimensional mono-layer is about 40% larger than the bulk value and that one of isolated atom according to Hund's rules can be even almost four times larger. The atomic magnetic moment is obviously very sensitive to the atomic arrangement in its vicinity and to local chemical composition. It should be emphasized that an important parameter for thin films is thus local strain.

Table 1

Magnetic moments in μ_B of an atom in the bulk of the crystal (bcc Fe and hcp Co), on the external free surface, in the two-dimensional mono-layer, in the one-dimensional atomic chain and of a free isolated atom

	bulk	surface	mono-layer	chain	free atom
Fe [5]	2.25	2.98	3.20	3.36	4.00
Co [6]	1.73	1.89		2.20	6.63

Let us discuss a simple model of an iron film on the substrate where the atomic spacing parallel to the interface is given by the lateral atomic spacing of the substrate and the atomic separation in the perpendicular direction is taken as a free parameter [7]. The calculations of the total energy were performed for the initially bcc crystal homogeneously deformed along the bcc – fcc tetragonal (Bain's) transformation path at various atomic volumes. The fcc structure is reached at the c/a ratio equal to $\sqrt{2}$ when the tetragonal uniaxially deformed structure is attaining again cubic symmetry. Different magnetic states were considered: non-magnetic, ferromagnetic, single-layer and double-layer antiferromagnetic states where the magnetic moments in the three later states are either uniformly ordered or alternate on neighbouring single or double atomic cubic planes.

The regions of different favoured magnetic states possessing the lowest total energy are schematically shown in the two-dimensional diagram in Fig. 1 where the free parameters are c/a on the x -axis and the atomic volume V normalized by the value for the bcc equilibrium structure on the y -axis. For a substrate with a fixed atomic spacing a , the two parameters $x=c/a$ and $y=a^2c/a_{\text{bcc}}^3=kx$ are related by the straight line, $k = a^3/a_{\text{bcc}}^3$ where a_{bcc} is the bcc lattice parameter. The favoured state can be predicted as the point corresponding to the lowest energy along this straight line.

The equilibrium bcc magnetic state ($c/a = 1$, $V = 1$) is ferromagnetic and the region of the antiferromagnetic states is located around $c/a = 1.5$ for compressed atomic volumes $V < 0.95$. The single-layered antiferromagnetic region is enveloped by the double-layered one. The results for various substrates are in a good agreement with the experiments as demonstrated in [7] despite the model simplifications. Let us recall that the thickness of the iron film is not considered, only the coherent relationship between the substrate and film is assumed. It indicates that the nature of magnetic state of the system is well captured in spite of omission of the inhomogeneities at the free surface and film/substrate interface.

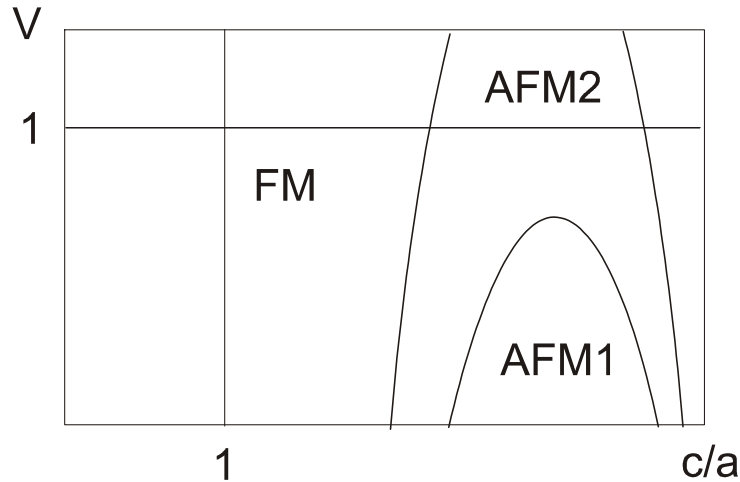


Fig. 1. Occurrence of different magnetic states at homogeneously deformed iron. c/a on the x -axis indicates the magnitude of the tetragonal deformation at given atomic volume and V on the y -axis the atomic volume normalized by the value for the bcc structure. FM, AFM1 and AFM2 are ferromagnetic, single-layer and double-layer antiferromagnetic states, respectively.

Misfit Dislocations

The main assumption of the preceding section was a coherent interface between the film and substrate. The condition of homogeneous structure of the film is fulfilled only when its thickness is smaller than certain critical width h_c when the homogeneously deformed layer has lower energy than the layer containing misfit dislocations at the film/substrate interface. Very thin films are fully pseudomorphic to the substrate, i.e., their structure can be entirely deduced from the substrate surface. Let us notice that the elastic strains can reach very high magnitudes in such thin films.

The elastic energy of a film having the width h is equal to $h M \varepsilon^2$ where M is the biaxial elastic modulus and ε elastic strain [8]. Assuming a square grid dislocation array with the dislocation spacing d , the energy per unit area of the interface can be evaluated as $2/d G b^2$ where G is shear modulus and b interfacial dislocation Burgers vector [9]. When the dislocations fully accommodate the lattice misfit between the film and substrate then $d = b/\varepsilon$ and the critical film width can be estimated as $h_c = 2Gb/M\varepsilon$, i.e., it is equal to the dislocation spacing multiplied by the ratio of elastic constants $2G/M$.

Strain relaxation in thin layers is of fundamental importance in both functional as well as structural materials. It determines morphological stability of layers essential for the production of electronic devices and plays a crucial role for the mechanical properties as well.

As an example let us discuss misfit dislocations compensating lattice misfit between different variants of the $L1_0$ structure in TiAl intermetallics [10]. When the plastic deformation has to be

transmitted across the interface, the incoming lattice dislocations interact with the interface misfit dislocations, and the strength of the interface, as an obstacle for dislocation motion, may depend on the actual arrangement of interface dislocations. The dislocation structure of an interface is always determined by the exact crystallographic relationship of the joint crystals. If there is a misfit between atomic planes in contact it can be in principle fully compensated by certain strain. The misfit arising from the difference of the lattice parameters of two isomorphic structures is accommodated by the edge dislocations producing extension on one side of the interface and contraction on the other side. The shear misfit type, which occurs on the lamellar interfaces in TiAl, can be compensated by screw dislocations, but the arrays of screw dislocations can cause a twist misorientation without any misfit as well. A required shear deformation can result from several dislocation networks differing by small additional misorientations about the axis perpendicular to the interface. In other words, the same strain tensor can be obtained by shears in different directions. In fact, it has been demonstrated experimentally for TiAl [10-19] that the misfit of certain magnitude can indeed be accommodated by various dislocation networks.

Three qualitatively different displacement fields at the interface can be distinguished: *expansion* or *contraction* in two perpendicular directions, *shear* equivalent to the expansion in one direction combined with the contraction in the perpendicular direction and *rotation* of one crystal with respect to the other one separated by the interface. The strain is distributed across the interface according to the elastic properties of the two media, it can be localized essentially only in one crystal when the other crystal is strongly harder. However, in the case of the interfaces between different TiAl variants with the identical elastic constants the strain will be symmetrically distributed in the two misoriented crystals.

The same shear deformation can be caused by the set of parallel screw dislocations in one direction or by another set in the perpendicular direction or by a combination of several dislocation arrays [10]. It can be shown that the crystallographic relationships of the two crystals for the perpendicular shears differ by a small rotation about the axis perpendicular to the interface, i.e., the later configuration is a superposition of the former configuration and a small angle twist boundary. Consequently, the lattice dislocations can react differently with diverse dislocation interfacial structures.

The interfaces are obviously efficient obstacles for dislocation motion. Dislocation processes taking place at the interfaces have been recently studied by *in situ* [20,21] and *post mortem* [22,23] electron microscopy. It was found, for example, that the strain of an incoming twin formed by the $1/6\langle 112 \rangle$ Shockley partials can be transferred to the neighbouring lamella across the 120° interface by the ordinary- and super-dislocations according to the reaction

$$6 \frac{1}{6}\langle 112 \rangle^I = 2 \frac{1}{2}\langle 110 \rangle^{II} + \langle 101 \rangle^{II} . \quad (I)$$

Since the Burgers vectors belong to two different crystals separated by the interface, the expression above indicates only the number and types of dislocations but not the specific crystallographic directions. The dislocations propagate along the $\{111\}$ plane in continuation of the initial glide plane. Another reaction can be written for the transition across the twin (180°) interface

$$3 \frac{1}{6}\langle 112 \rangle^I = 3 \frac{1}{6}\langle 112 \rangle^{II} + \frac{1}{2}\langle 110 \rangle^{II} + \frac{1}{2}\langle 110 \rangle^I . \quad (II)$$

In this case the dislocations lie on the mirror symmetric glide planes. It is seen that the motion of Shockley partials of twinning is accompanied in both lamellae by the glide of ordinary dislocations. For the difficulties to observe *in situ* what is happening at the interfaces, the role of interface dislocations was analysed *post mortem* and the following reaction was proposed

$$3 \frac{1}{6} \langle 112 \rangle^I = 3 \frac{1}{6} \langle 112 \rangle^{II} + 2 \frac{1}{2} \langle 110 \rangle^{II} + 2 \frac{1}{6} \langle 112 \rangle^{I-II}. \quad (\text{III})$$

The incoming and outgoing planes are mirror symmetric with respect to the twin interface. Notice that the last term represents interfacial dislocations with the Burgers vector parallel to the interface. Propagation of outgoing Shockley partials is again associated with the ordinary dislocations. It can be concluded that the twinning is linked with the motion of ordinary dislocations arising from the reactions at the interfaces during the transfer of plastic deformation.

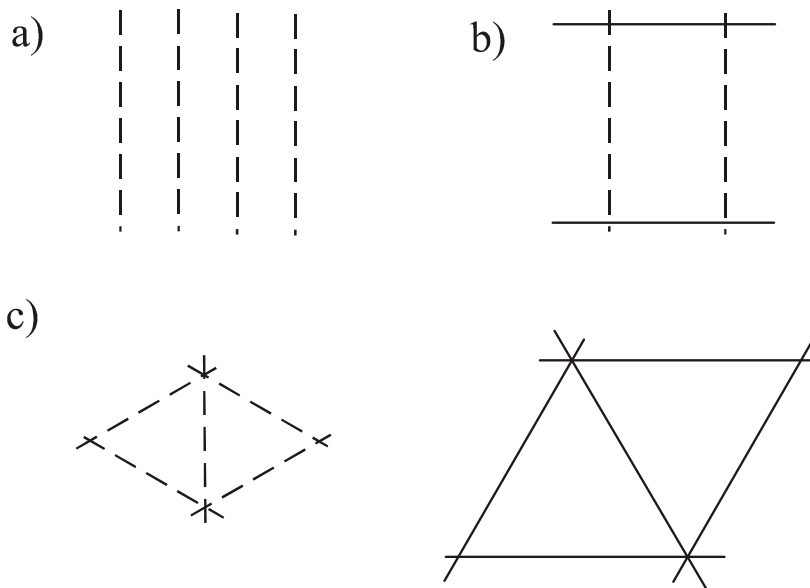


Fig. 2. Different arrays of interfacial dislocations compensating the misfit of shear type. Dashed lines represent $\frac{1}{6}\langle 112 \rangle$ dislocations, full lines $\frac{1}{2}\langle 110 \rangle$ dislocations.

It has been demonstrated in [10,19] that the misfit caused by the tetragonality of the $L1_0$ structure on the 120° and 60° (pseudotwin) interfaces can be compensated by the networks of interfacial dislocations of various types. In principle, just one set of screw dislocations (Fig. 2a) would be sufficient, but the same misfit of shear type can be compensated also by two (Fig. 2b) or three (Fig. 2c) dislocation arrays. The Burgers vectors of interfacial dislocations lie at the interface. An array of dislocations with the Burgers vector perpendicular to the interface would give rise to a tilt deviation from this interface of special character and such deviation is likely to increase the interfacial energy.

The interfacial dislocations are apparently mobile along the interface, and can thus increase the flexibility of plastic deformation. The macroscopic measurements [24,25] show that the strain in the lamellae is parallel to the interfaces in the samples loaded along the lamellae, i.e., the resulting strain is parallel to the plane with zero resolved shear stress. This is a consequence of the fact that the deformation modes inclined to the lamellae are combined in such a way to give strain not interfering with the interfaces.

Grain Boundary Classification

Grain boundaries are characterized by the mutual rotation of two adjoint crystals and by the normal to the boundary plane. Moreover, in addition to these extrinsic parameters, the intrinsic factors

describing unequal boundary atomic structures such as a relative translation of the two grains has to be considered. A large attention was paid to the symmetrical boundaries as their special structures and properties were anticipated. A geometrical classification of symmetrical boundaries for the fcc as well as bcc bicrystals was proposed in [26] on the basis of interplanar spacing that is related to the atomic density on the planes parallel to the boundary. The classification starts from the most close-packed planes and generates the normals to the symmetrical boundaries covering gradually the whole space of plane orientations. To complete all possible grain boundary types, geometry of asymmetrical boundaries was examined in [27].

Grain boundaries can be divided into three classes: (i) high energy *general* grain boundaries with a tendency to intergranular fracture, (ii) low energy *singular (special)* grain boundaries with the properties closer to those of unperturbed crystal, and (iii) transitive *vicinal* grain boundaries [28]. Three steps can be distinguished in the experimental characterization of polycrystals: determination of (a) the grain orientations used in texture analysis, (b) the mutual rotations of neighbouring crystals and (c) the normals to grain boundary surfaces. The reciprocal density of coincidence sites (parameter Σ) that is directly related to the grain rotation is a main characteristics of grain boundaries generally used in literature. The approach of *Grain Boundary Engineering* trying to increase the portion of special boundaries with better properties is often based on Σ values [29,30]. However, according to our findings also asymmetrical boundaries with very large Σ values can display special behaviour. Notice that quite different properties can be detected for grain boundaries with the same crystal misorientation, and hence the same Σ values, when the boundary plane is differently inclined [31].

The orientation dependence of grain boundary energy for symmetrical boundaries in bcc metals was studied using many-body as well as empirical potentials in [32]. While essentially only $\Sigma 5$ boundaries on $\{013\}$ and $\{012\}$ deviate from a smooth curve of general high-angle boundaries for the $[100]$ rotation axis, more pronounced cusps for $\Sigma 3$ $\{112\}$ and $\Sigma 11$ $\{332\}$ are detected for the $[110]$ rotations, similarly to fcc metals where the special symmetrical boundaries are on $\{111\}$ and $\{113\}$.

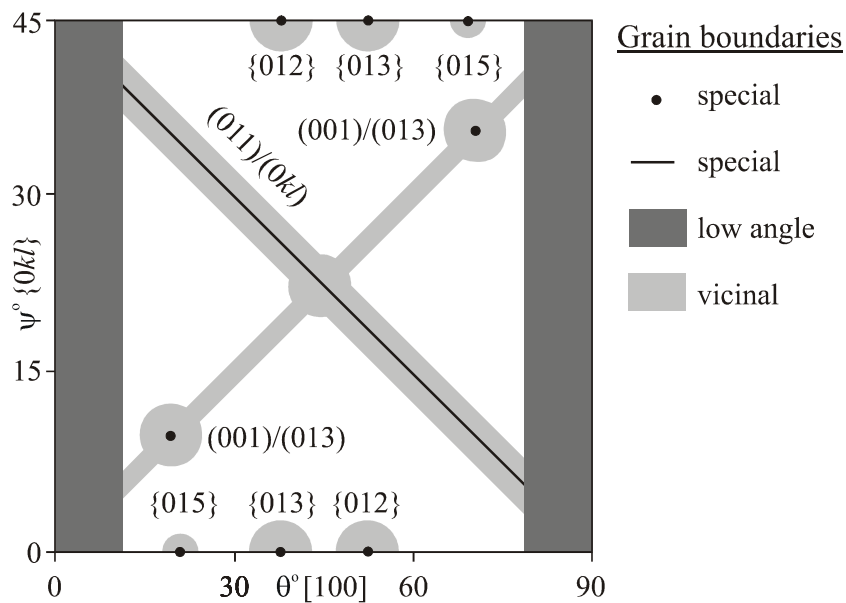


Fig. 3. Classification of $[100]$ tilt grain boundaries in α -iron.

The anisotropy of grain boundary segregation is in agreement with the following classification of the [100] tilt grain boundaries in α -iron [33] (see Fig. 3):

- symmetrical {015}, {013} and {012}, and (001)/(013) and all (011)/(0kl) asymmetrical boundaries are *special*;
- boundaries in the vicinity of special grain boundaries and all (001)/(0kl) asymmetrical grain boundaries are *vicinal* except the (001)/(013) and (001)/(011) interfaces;
- all other grain boundaries with the misorientation larger than about 10° – 15° are *general*.

Although the special {012}, {013} and {015} symmetrical grain boundaries possess – in agreement with the Coincidence Site Lattice model – low values of Σ (5, 5 and 13, respectively), a large discrepancy between this and traditional classification is found for asymmetrical interfaces. For example, the (001)/(011) non-coincidence ($\Sigma \rightarrow \infty$) grain boundary is special. The $\Sigma 5$ 36.9° [100] misorientation relationship covers all classes of grain boundaries, special {013}, (011)/(017) and {012}; vicinal (001)/(034); and general (018)/(047) and (0 3 11)/(097). It is clear from these examples, that an uncritical acceptance of Σ as a criterion for special grain boundary behaviour is misleading especially in the case of asymmetrical interfaces.

Grain Boundary Engineering

A specific arrangement of low-angle and/or special grain boundaries can prevent intergranular crack propagation to a large extent, and the fracture strength becomes then comparable with that of transgranular cleavage. Generalizing this idea, Watanabe proposed the concept of grain boundary design for polycrystals (*Grain Boundary Engineering*) [29,34] to produce material with grain boundaries of such character and distribution that results in significant improvement of its properties.

To apply this concept, it is necessary to consider various parameters of a large spectrum of grain boundaries such as boundary area and width, their junctions, grain size and shape, interfacial faceting, phase formation; type, character and structure of grain boundaries, chemical composition and segregation, and energetic parameters [34]. The production of polycrystal with better properties is based on various kinds of thermo-mechanical treatment including classical strain/anneal techniques that are used to increase the frequency of special (twin) grain boundaries that frequently interrupt the network of general interfaces in a new microstructure thus increasing the resistance of material against intergranular brittle fracture. Formation of new microstructure can be caused by faster motion of special interfaces during recrystallization as compared to general ones. Newly developed processes may also adopt annealing in magnetic field that retards recrystallization and substantially increases the frequency of the low-angle and special grain boundaries as it was found in Fe–9%Co alloy [35].

Summary

Selected properties of material interfaces were briefly reviewed. The attention was focused on magnetic properties of thin films, the dislocation structures compensating crystal misfit and new more complete classification of grain boundaries. It should be emphasized that certain asymmetrical grain boundaries show special behaviour comparable with low-value Σ special boundaries. A better knowledge of behaviour of all possible types of grain boundaries is still highly desirable.

Acknowledgement

The authors acknowledge the financial support of the Czech Science Foundation under grant No. 202/04/2016 and of the Grant Agency of the Academy of Sciences (No. A1041302/2003).

References

1. Kurishita, H., Kuba, S., Kubo, H. and Yoshinaga, H.: *Trans. JIM* **26** (1985), 332.
2. Kurishita, H., Oishi, A., Kubo, H. and Yoshinaga, H.: *Trans. JIM* **26** (1985), 341.
3. Kurishita, H. and Yoshinaga, H.: *Mater. Forum* **13** (1989), 161.
4. Tsurekawa, S., Tanaka, T. and Yoshinaga, H.: *Mater. Sci. Eng. A* **176** (1994), 341.
5. Freeman, A.J. and Wu, R.Q.: *J. Magn. Magn. Mater.* **104-107** (1992), 1.
6. Ney, A., Pouloupoulos, P. and Beberschike, K.: *Europhys. Lett.* **54** (2001), 820.
7. Friák, M., Šob, M. and Vitek, V.: *Phys. Rev. B* **63** (2001), 052405_4pp.
8. Nix, W.D.: *Metall. Trans. A* **20** (1989), 2217.
9. Stokes, R.J. and Evans, D.F.: *Fundamentals of Interfacial Engineering* (Wiley -VCH, New York, 1997).
10. Paidar, V., Zghal, S. and Couret, A.: in *High-Temperature Ordered Intermetallic Alloys VIII*, ed. E.P. George, M.J. Mills and M. Yamaguchi. *Mater. Res. Soc. Symp. Proc. Vol. 552*. Warrendale, PA, 1999), p. KK3.2.1.
11. Zhao, L. and Tangri, K.: *Phil. Mag. A* **64** (1991), 361.
12. Zhao, L. and Tangri, K.: *Acta Metall. Mater.* **39** (1991), 2209.
13. Zhao, L. and Tangri, K.: *Phil. Mag. A* **65** (1992), 1065.
14. Hazzledine, P.M., Kad, B.K., Fraser, H.L. and Dimiduk, D.M.: in *Intermetallic Matrix Composites II*, ed. D.B. Miracle, D.L. Anton and J.A. Graves. *Mater. Res. Soc. Proc. Vol. 273*. Pittsburgh, PA, 1992), p. 81.
15. Kad, B.K. and Hazzledine, P.M.: *Phil. Mag. Lett.* **66** (1992), 133.
16. Kad, B.K. and Fraser, H.L.: *Phil. Mag. Lett.* **68** (1993), 21.
17. Inkson, B.J. and Humphreys, C.J.: *Phil. Mag. A* **73** (1996), 1333.
18. Inkson, B.J. and Ruhle, M.: *Phil. Mag. Lett.* **74** (1996), 317.
19. Paidar, V., Zghal, S. and Couret, A.: *Mater. Sci. Forum* **294-296** (1999), 385.
20. Zghal, S., Coujou, A. and Couret, A.: *Phil. Mag. A* **81** (2001), 345.
21. Zghal, S. and Couret, A.: *Phil. Mag. A* **81** (2001), 365.
22. Gibson, M.A. and Forwood, C.T.: *Phil. Mag. A* **80** (2000), 2747.
23. Forwood, C.T. and Gibson, M.A.: *Phil. Mag. A* **80** (2000), 2785.
24. Kishida, K., Inui, H. and Yamaguchi, M.: *Phil. Mag. A* **78** (1998), 1.
25. Kim, M.-C., Nomura, M., Vitek, V. and Pope, D.P.: in *High-Temperature Ordered Intermetallic Alloys VIII*, ed. E.P. George, M.J. Mills and M. Yamaguchi. *Mater. Res. Soc. Proc. Vol. 552*. Warrendale, PA, 1999), p. KK3.1.1.
26. Paidar, V.: *Acta Metall.* **35** (1987), 2035.
27. Paidar, V.: *Phil. Mag. A* **66** (1992), 41.
28. Sutton, A.P. and Balluffi, R.W.: *Interfaces in Crystalline Materials* (Clarendon, Oxford, 1995).
29. Watanabe, T.: *Res. Mech.* **11** (1984), 47.
30. Lehecky, E.M., Palumbo, G. and Lin, P.: *Metall. Mater. Trans. A* **29** (1998), 3069.
31. Lejček, P., Paidar, V., Adámek, J. and Hofmann, S.: *Acta Mater.* **45** (1997), 3915.
32. Wolf, D.: *Phil. Mag. A* **62** (1990), 447.
33. Lejček, P., Hofmann, S. and Paidar, V.: *Acta Mater.* **51** (2003), 3951.
34. Watanabe, T.: in *Grain Boundary Engineering*, ed. U. Erb and G. Palumbo. (Canadian Institute of Mining Metallurgy and Petrol, Montreal, 1993), p. 57.
35. Watanabe, T., Suzuki, Y., Tanii, S. and Oikawa, H.: *Phil. Mag. Lett.* **62** (1990), 9.

Observation of lattice defects and nondestructive evaluation of fatigue life in FeAl and Ni₃Al based alloy by means of magnetic measurement

Yukichi Umakoshi^{1, a} and Hiroyuki Y. Yasuda^{2, b}

¹Department of Materials Science and Engineering, Graduate School of Engineering, Osaka University, 2-1, Yamada-oka, Suita, Osaka 565-0871, Japan

²Research Center for Ultra-High Voltage Electron Microscopy, Osaka University, 7-1, Mihogaoka, Ibaraki, Osaka, 567-0047, Japan

^aumakoshi@mat.eng.osaka-u.ac.jp, ^bhyyasuda@mat.eng.osaka-u.ac.jp,

Keywords: fatigue, lattice defect, magnetic property, nondestructive evaluation, intermetallic compound, fracture, deformation

Abstract. A magnetic technique was applied to examine cyclic deformation behavior and deformation damage in ordered FeAl and Ni₃(Al,Ti) single crystals. The fatigue lifetime of FeAl was evaluated by an abrupt increase in spontaneous magnetization. The morphology of γ precipitates in Ni₃(Al,Ti) during annealing and deformation was examined by changes in spontaneous magnetization and coercive force.

1. Introduction

Magnetic properties of ferromagnetic materials are known to correlate with lattice defects. A transition between ferromagnetism and paramagnetism by plastic deformation often occurs in several types of intermetallics such as Pt₃Fe, Ni₃Mn, Pt₃Co, Ni₃Fe, Ni₃Al, FeAl and Fe₃Al [1,2]. One of the authors [2,3] previously reported that the deformation-induced magnetization in FeAl is caused by the atomic environment and magnetic coupling changes near an anti-phase boundary (APB) between two superpartials. Since magnetic susceptibility, coercive force and high-field susceptibility are also sensitive to the lattice defects, a magnetic technique has been applied for nondestructive evaluation of mechanical damage in ferromagnetic materials and observation of lattice defects. In this paper, we quantitatively examine the quantity of APBs in cyclically deformed FeAl single crystals and try a nondestructive evaluation of the fatigue lifetime using a magnetic technique.

Ni-base superalloys which consist of L1₂ ordered γ' and disordered γ phases have been used as a superior high-temperature structural material for gas turbine and jet engine turbine blades. The γ' phase shows a weak paramagnetism and slight change in magnetization even after strong deformation [4]. However, since the γ phase is ferromagnetic and the magnetic property is strongly influenced by deformation, the deformation behavior is expected to be examinable through change in the magnetic property of γ phase. We also report deformation behavior of Ni₃(Al,Ti) single crystals composed of γ' matrix and small γ precipitates focusing on change in magnetic property of the precipitates.

2. Experimental procedure

FeAl containing 40at%Al, and Ni₃(Al,Ti) containing 18at%Al and 4at%Al single crystals were grown by a floating zone method at a rate of 5mm/h in a purified argon gas flow. FeAl crystals were annealed at 698K for 100h to eliminate frozen-in vacancies after homogenization at 1373K for 48h. Plastic strain ($\Delta\varepsilon_p$) controlled fatigue tests for specimens with [149] loading axis were performed in a tension-compression mode at room temperature at an average strain rate of $3 \times 10^{-4} \text{s}^{-1}$. A stress controlled fatigue test was also performed with 300MPa. After the fatigue tests, deformation

substructure was observed by a TEM operated at 200kV. Deformation-induced magnetization was measured at 77K by a vibrating sample magnetometer (VSM).

$\text{Ni}_3(\text{Al,Ti})$ crystals were aged at 1073K to precipitate the disordered γ phase in γ' matrix after homogenization at 1423K for 168h and subsequent solution treatment at 1423 for 24h. Specimens for compression or fatigue tests have a $[\bar{1}49]$ loading axis. Tension-compression fatigue tests were performed at total strain amplitude of 0.2% and initial strain rate of $3.0 \times 10^{-4} \text{ s}^{-1}$. Morphology of γ precipitates and dislocation structure were observed using a TEM. Magnetic measurements were made by VSM at 77K. To examine temperature dependence of magnetization, samples were cooled with or without a magnetic field of 100Oe and the applied magnetic field during the measurement was also 100Oe.

3. Results and Discussion

3-1. Magnetic observation of lattice defects and evaluation of fatigue lifetime in FeAl.

The maximum stress rapidly increased and the specimen fractured after an initial gradual increase at $\Delta \varepsilon_p = 0.025 \sim 0.100\%$. The fatigue lifetime decreased with increase in $\Delta \varepsilon_p$. According to TEM observation, a $\langle 111 \rangle$ superlattice dislocation is dissociated into two superpartials bound by an APB ribbon at the early stage of fatigue. In the hardly fatigued specimen, APB tubes were observed together with numerous dipoles, loops and point defect clusters. APB tubes were annihilated but APB ribbons remained after annealing at 573K for 2h. Dislocation density in cyclically deformed specimens was measured by counting the number of intersections between dislocations and a square mesh. The undeformed FeAl specimen shows paramagnetism but the magnetization curve is not straight at low magnetic field because of the appearance of magnetization after deformation. A paramagnetic-to-ferromagnetic transition occurs by plastic deformation. The spontaneous magnetization (M_s) in deformed samples is obtained by extrapolation of the linear part at higher magnetic field back to the zero field.

Figure 1 shows change in spontaneous magnetization (M_s) of FeAl single crystals as a function of dislocation density (ρ) during fatigue and after annealing. M_s increases almost linearly up to $7 \times 10^{13} \text{ m}^{-2}$ and then shows an abrupt increase with increasing ρ . After annealing at 573K for 2h, M_s rapidly decreases and shows a linear relation with ρ . Since APB tubes are annihilated by annealing, the difference of M_s between an as-deformed sample and an annealed one after deformation is due to these tubes. Magnetic properties in Fe-Al ordered alloys are known to depend strongly on their alloy composition. In the composition range between 35 and 50at%Al a paramagnetism is observed, while ferromagnetism appears in a composition less than 35at%Al [5]. However, a paramagnetic-to-ferromagnetic transition occurs even for more than 35at%Al.

In FeAl ordered alloys with the B2 structure, Fe-Al bonds exist but there are no Fe-Fe and Al-Al bonds at the first nearest neighbors. A $\langle 111 \rangle$ superlattice dislocation is dissociated into two superpartials on $\{110\}$ plane. An APB can be created due to atomic displacements by a $1/2 \langle 111 \rangle$ superpartial. As a result of formation of the APB, Fe-Fe bonds are introduced at the first nearest neighbors and the Fe-Fe bond chains align two dimensionally on the APB as shown in Figure 2. Magnetization is due to formation

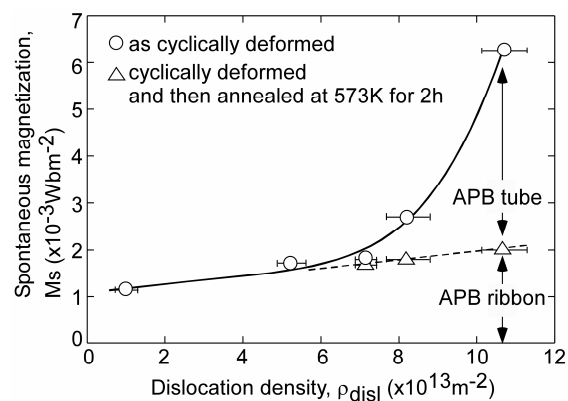


Fig.1 Variation in spontaneous magnetization of fatigued FeAl single crystals and annealed ones after fatigue as a function of dislocation density.